Supporting Information

Cu^{2+}-Activatable Fluorescence and Chemiluminescence Dual-Mode Sensing Platform for Visual Detection of Thiram

Pan Zhu[a], Yuanyu Tang[a], Yu Tang[b], Yating Xu[a], Shaojing Zhao[a], Chaoyi Yao[a], Benhua Wang[a], Xiangzhi Song[a], Minhuan Lan[a,] *

[a]College of Chemistry and Chemical Engineering, Central South University, Changsha, 410083, P. R. China
[b]Department of Gastroenterology, The Third Xiangya Hospital of Central South University, Changsha, 410013, P. R. China

1. Experimental General

Instruments and materials. Unless otherwise stated, all solvents and chemicals were purchased from commercial suppliers in analytical grade and used without further purification. Ultrapure water was used in all spectroscopic studies. The ^{1}H and ^{13}C NMR spectra were recorded on a Bruker AVANCE III 400 or 500 spectrometer, using TMS as an internal standard. High resolution mass spectrometry data was obtained from the Bruker compact instrument. Absorption spectra were collected on a Shimadzu UV-2600 spectrophotometer, fluorescence and chemiluminescence spectra were performed on a Hitachi F-7000 fluorescence spectrophotometer. Chemiluminescence images were collected by virtue of Aniview 100 IVIS system.

Theoretical calculation. The optimized molecular geometry of **Ac-Do-Py** were performed via the Gaussian 16, Revision C.01[1], at a B3LYP/6-311G(d) level. The electrostatic potential (ESP) was calculated based on the optimized molecular geometry and analyzed with Multiwfn[2,3]. The Visual Molecular Dynamics program was used to plot the color-filled iso-surface graphs to visualize the maps of ESP surfaces[4].

Spectrum test. The UV-Vis absorption, fluorescence (λ_{ex} = 400 nm), and chemiluminescence spectra of **Ac-Do-Py** were recorded using UV-2600 and F-7000 spectrometers, respectively.

Fluorescence kinetics. 5 μM **Ac-Do-Py** in HEPES (pH = 7.4) with Cu^{2+} (30 μM) was placed in the F-7000 spectrometer. Fluorescence spectra were acquired at an interval of 5 min.

Chemiluminescence kinetics. 5 μM **Ac-Do-Py** in HEPES (pH = 7.4) with Cu^{2+} (30 μM) was placed in the AniView 100 imaging device. Chemiluminescence signals were recorded for 40 min. Unless otherwise stated, chemiluminescence imaging parameters were as follows: bioluminescence mode, open channel, automatic exposure, and field of view: D. Regions of interest (ROI) for image analysis were defined using AniView software.

Detection of thiram in solution. First, Cu^{2+} (30 μM) was added to HEPES solutions (pH = 7.4) containing thiram at different concentrations (0, 10, 20, 40, and 60 μM). The mixture was incubated for 60 min. Then, **Ac-Do-Py** (5 μM) was added to the thiram/Cu^{2+} solution. Fluorescence spectra (λ_{ex} = 420 nm) were recorded 3 min after the addition of the probe. Chemiluminescence images were captured after 10 min using the AniView 100 device.

In situ **detection of thiram on actual fruits.** Thiram (60 μM) was sprayed onto the surfaces of orange peel, strawberry leaves, and cherry leaves. Then, Cu^{2+} (30 μM) was sprayed onto the fruit samples and incubated for 30 min followed by **Ac-Do-Py** (5 μM). Immediately after completing these steps, the samples were subjected to chemiluminescence imaging using the IVIS system.

2. Synthetic Methods.

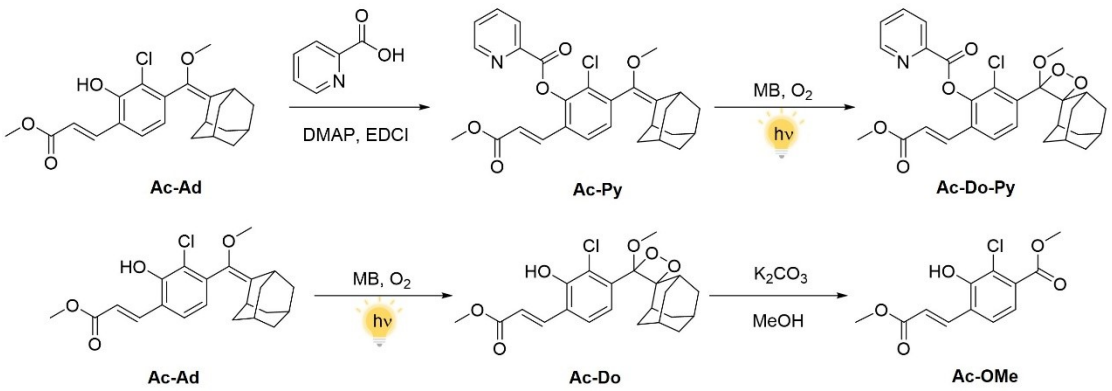

Scheme S1 Synthesis routes of **Ac-Do-Py** and **Ac-OMe**.

Synthesis of Ac-Py

Ac-Ad was synthesized according to the literature[5].

Ac-Ad (50 mg, 0.13 mmol), 2-pyridinecarboxylic acid (24 mg, 0.195 mmol), 4-Dimethylaminopyridine (4.8 mg, 0.04 mmol), and 1-(3-Dimethylaminopropyl)-3-ethylcarbodiimide hydrochloride (37 mg, 0.195 mmol) were dissolved in 8 mL of dry dichloromethane (DCM). The above mixture was stirred at room temperature for 5 h under nitrogen atmosphere, and then diluted with DCM and washed with brine. The organic phase was dried over anhydrous Na_2SO_4, and then the crude product was purified by silica gel column chromatography with petroleum ether/ethyl acetate (PE/EA) = 10/3 as the eluent to obtain an off-white solid (45 mg, 74% yield). ^{1}H NMR (400 MHz, $CDCl_3$, ppm) δ = 8.91 (d, J = 3.9 Hz, 1H), 8.34 (dt, J = 7.8, 1.1 Hz, 1H), 7.98 (td, J = 7.8, 1.7 Hz, 1H), 7.76 (d, J = 16.0 Hz, 1H), 7.63 (ddd, J = 7.7, 4.7, 1.2 Hz, 1H), 7.58 (d, J = 8.1 Hz, 1H), 7.27 (s, 1H), 7.25 (s, 1H), 6.53 (d, J = 16.0 Hz, 1H), 3.74 (s, 3H), 3.34 (s, 3H), 3.28 (s, 1H), 2.13 (s, 1H), 1.88 (dt, J = 40.9, 24.8 Hz, 12H). ^{13}C NMR (101 MHz, $CDCl_3$, ppm) δ = 166.68, 162.44, 146.39, 146.33, 138.94, 137.98, 137.40, 137.34, 132.96, 129.69, 129.06, 128.99, 127.86, 126.28, 125.15, 121.41, 57.26, 51.79, 39.26, 39.04, 38.59, 37.04, 32.91, 29.77, 28.28. HRMS (ESI) m/z: $[M + H]^+$ calcd for $C_{28}H_{28}ClNO_5$, 494.1729; found, 494.1981

Synthesis of Ac-Do-Py

Ac-Py (15 mg, 0.03 mmol) and methylene blue (1 mg, 0.003 mmol) were dissolved in

10 mL of dry DCM. The mixture was allowed to cool to 0 °C and oxygen was bubbled into the solution under yellow light (50 W/cm^2) irradiation for 60 min. The **Ac-Do-Py** was obtained by silica gel column chromatography with PE/EA = 3/1 as the eluent (11 mg, 68% yield). ^{1}H NMR (500 MHz, $CDCl_3$, ppm) δ = 8.91 (ddd, *J* = 4.7, 1.7, 0.8 Hz, 1H), 8.33 (dt, *J* = 7.8, 1.1 Hz, 1H), 8.10 (d, *J* = 8.4 Hz, 1H), 7.98 (td, *J* = 7.7, 1.8 Hz, 1H), 7.79 - 7.70 (m, 2H), 7.64 (ddd, *J* = 7.7, 4.8, 1.2 Hz, 1H), 6.59 (d, *J* = 16.0 Hz, 1H), 3.75 (s, 3H), 3.24 (s, 3H), 3.01 (d, *J* = 4.5 Hz, 1H), 2.23 (d, *J* = 12.8 Hz, 1H), 2.05 (d, *J* = 4.2 Hz, 1H), 1.97 - 1.37 (m, 11H). ^{13}C NMR (126 MHz, $CDCl_3$, ppm) δ = 166.48, 150.35, 147.08, 146.00, 137.53, 136.86, 135.12, 130.90, 130.84, 128.06, 126.85, 126.39, 125.33, 122.65, 111.61, 96.43, 51.91, 49.80, 36.56, 33.90, 33.60, 32.21, 31.58, 31.51, 26.17, 25.73. HRMS (ESI) m/z: $[M + H]^+$ calcd for $C_{28}H_{28}ClNO_7$, 526.1628; found, 526.1899.

Synthesis of Ac-OMe

Ac-Ad (20 mg, 0.05 mmol) and methylene blue (2 mg, 0.006 mmol) were dissolved in 10 mL of dry DCM. The mixture solution was cooled to 0 °C and then oxygen was bubbled under yellow light (50 W/cm^2) irradiation. After the reaction is completed, **Ac-Do** (15 mg, 0.03 mmol) was directly obtained by silica gel column chromatography with PE/EA = 4/1 as the eluent. After that, **Ac-Do** was dissolved in 2 mL of methanol followed by addition of 10 mg of K_2CO_3. After completion, the solvent was removed under reduced pressure. the crude product was purified by silica gel column chromatography with PE/EA = 4/1 as the eluent to afford **Ac-OMe** as a white solid (6 mg, 62% yield). ^{1}H NMR (400 MHz, $CDCl_3$, ppm) δ = 7.93 (d, *J* = 16.2 Hz, 1H), 7.50 - 7.42 (m, 2H), 6.66 (d, *J* = 16.2 Hz, 1H), 3.94 (s, 3H), 3.82 (s, 3H).

3. Supplementary Figures

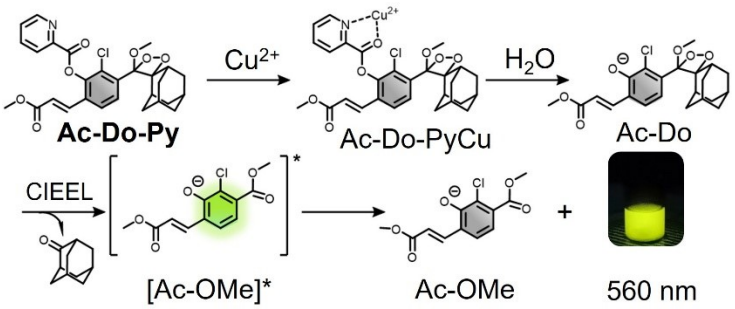

Fig. S1 Schematic illustration of the response mechanism of **Ac-Do-Py** towards Cu^{2+} and a photograph showing the generation of chemiluminescence under strong basic conditions.

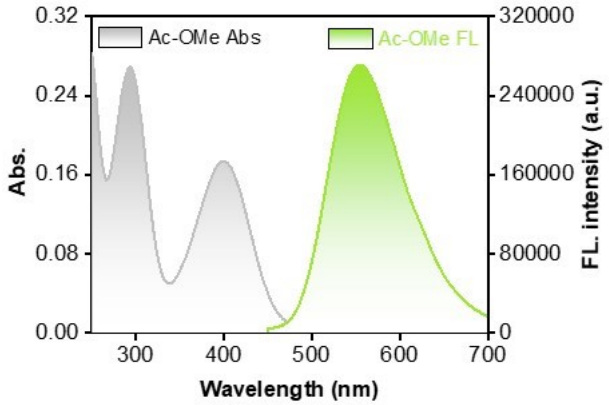

Fig. S2 Absorption and fluorescence spectra of **Ac-OMe** in HEPES (pH = 7.4, containing 10% DMSO).

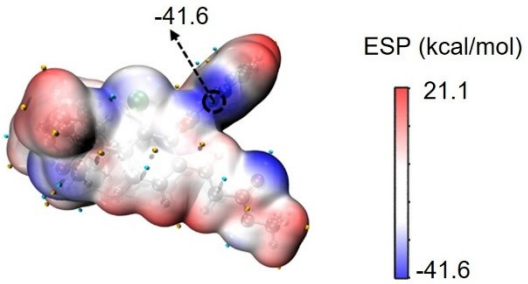

Fig. S3 ESP distribution of **Ac-Do-Py**.

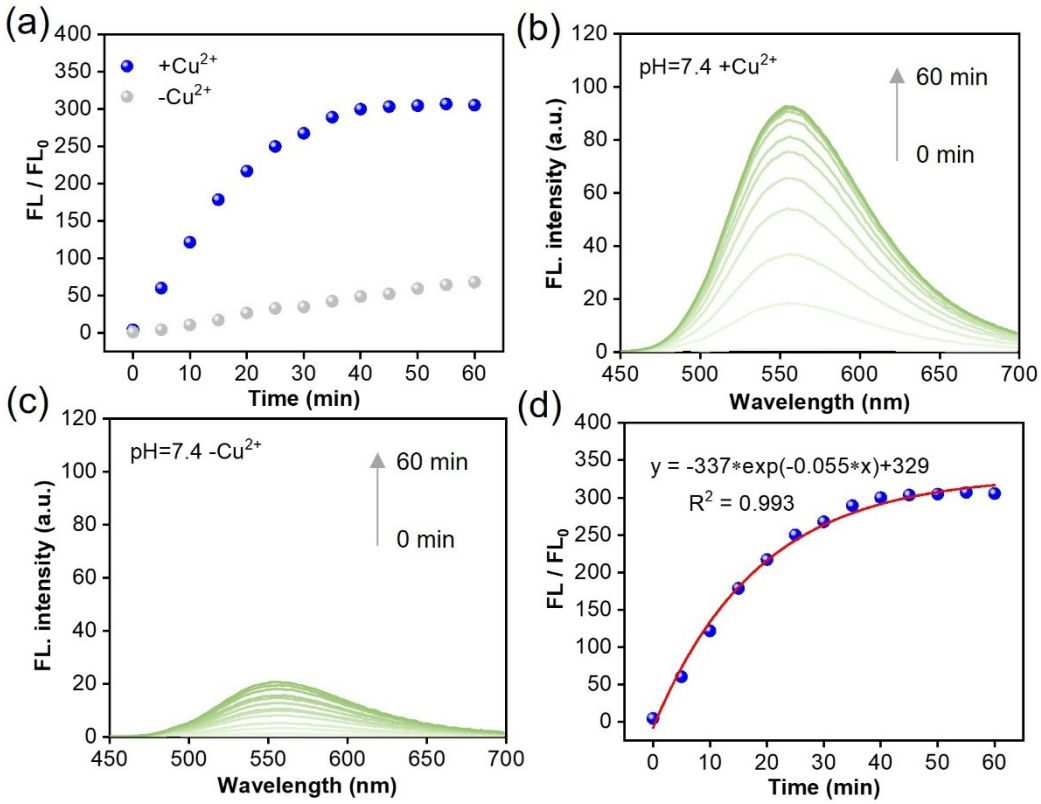

Fig. S4 (a) Fluorescence kinetics of **Ac-Do-Py** (5 μM) in HEPES buffer in the presence or absence of Cu^{2+}. Time-dependent fluorescence spectra of **Ac-Do-Py** (5 μM) in the presence (b) and absence (c) of Cu^{2+} (30 μM). (d) The fitting curve of the fluorescence kinetic data, which is in accord with a first-order equation with a rate constant (k) of 0.05 min^{-1} for the reaction between **Ac-Do-Py** (5 μM) and Cu^{2+} (30 μM).

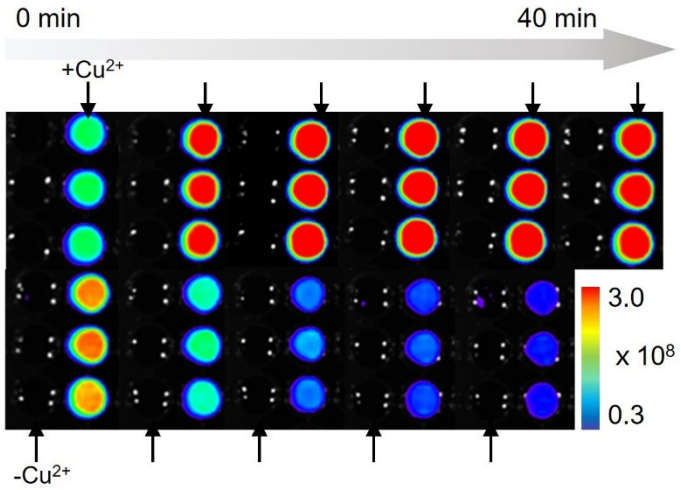

Fig. S5 Time-dependent chemiluminescence images of **Ac-Do-Py** (5 μM) in the presence of and absence of Cu^{2+} (30 μM)

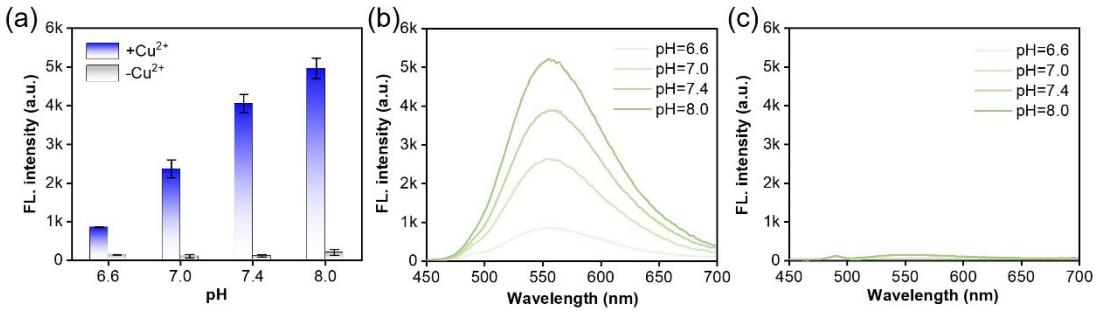

Fig. S6 (a) Fluorescence of **Ac-Do-Py** (5 μM) in the presence or absence of Cu^{2+} (30 μM) in HEPES buffers at different pH values. Fluorescence spectra of **Ac-Do-Py** (5 μM) in HEPES with different pH values in the presence (b) and absence (c) of Cu^{2+} (30 μM). Fluorescence spectra were collected after incubation with Cu^{2+} for 3 min.

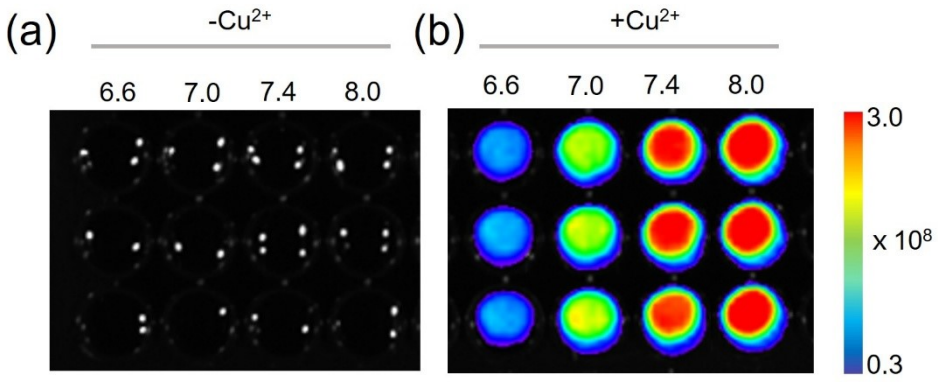

Fig. S7 Chemiluminescence images of **Ac-Do-Py** (5 μM) in HEPES with different pH values in the absence (a) and presence (b) of Cu^{2+} (30 μM). Chemiluminescence images were acquired after 10 min in the absence or the presence of Cu^{2+}.

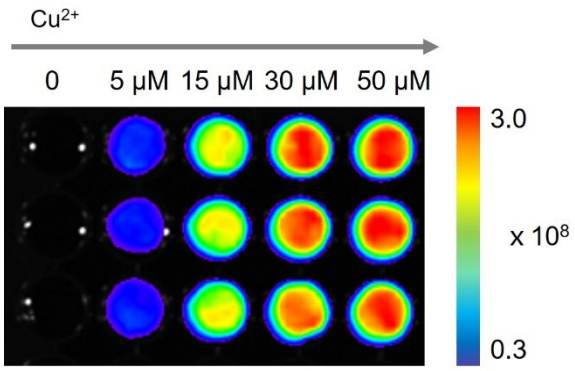

Fig. S8 Chemiluminescence images of **Ac-Do-Py** (5 μM) treated with different concentration of Cu^{2+}.

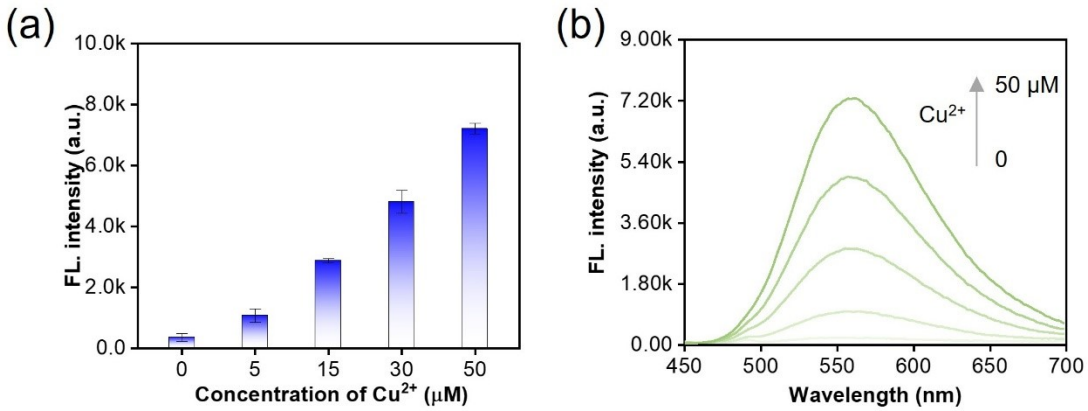

Fig. S9 (a) Fluorescence intensity and (b) spectra of **Ac-Do-Py** (5 μM) treated with different concentration of Cu^{2+}.

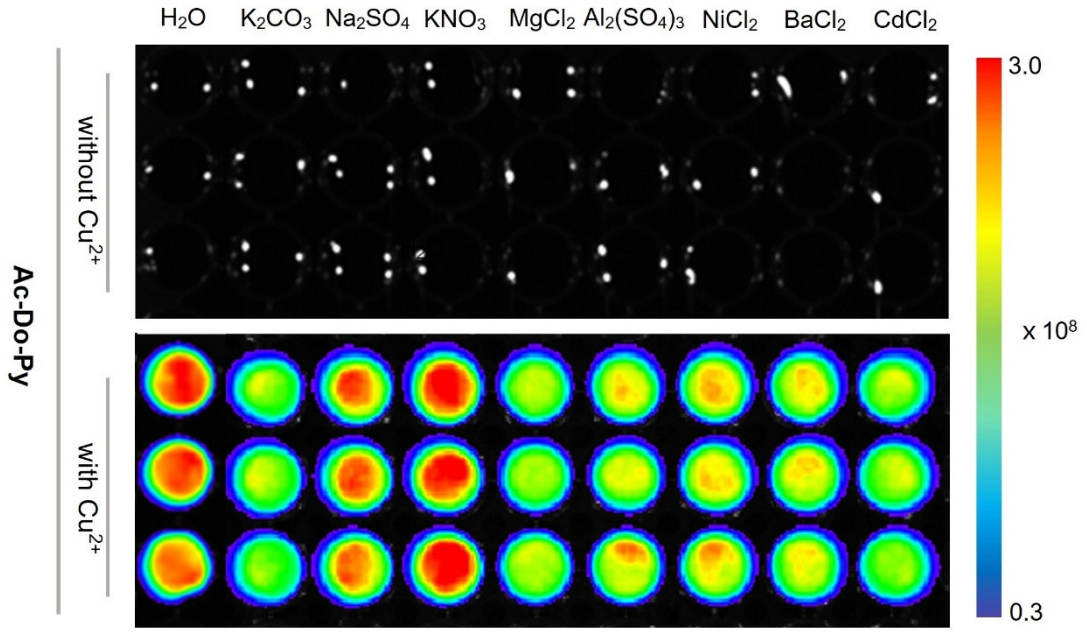

Fig. S10 Chemiluminescence images of **Ac-Do-Py** (5 μM) treated with various interferents in the absence or presence of Cu^{2+} for 10 min (Cu^{2+}: 30 μM, interferents: 100 μM).

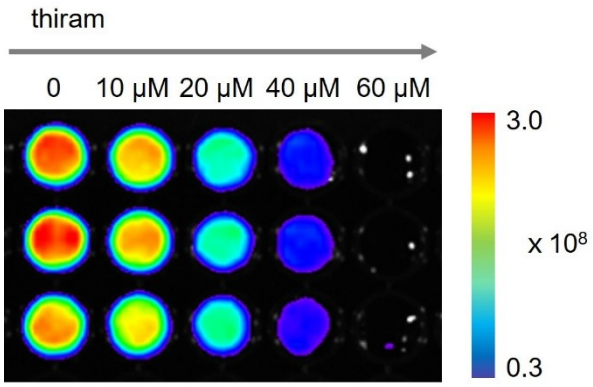

Fig. S11 Chemiluminescence images of **Ac-Do-Py** (5 μM)/Cu^{2+} (30 μM) and different concentration of thiram. (Chemiluminescence signal was acquired 10 min after addition of Cu^{2+}).

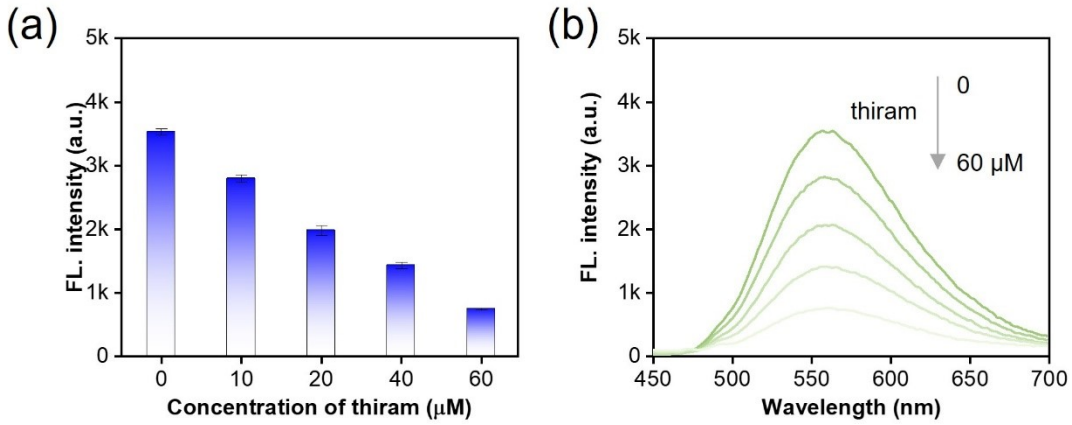

Fig. S12 (a) Fluorescence intensity and (b) spectra of **Ac-Do-Py** (5 μM)/Cu^{2+} (30 μM) and different concentration of thiram. (Fluorescence was collected 3 min after incubation with Cu^{2+}).

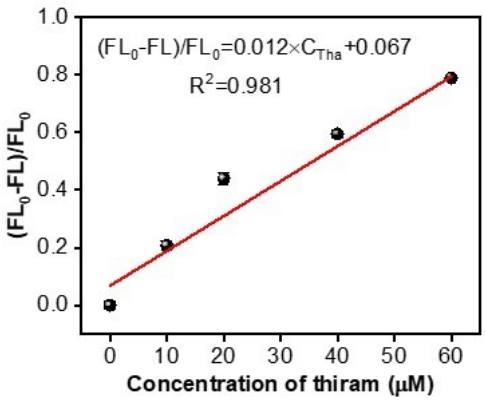

Fig. S13 Linear relationship between fluorescence quenching efficiency, (FL_0 - FL)/FL_0, and thiram

concentration. FL and FL_0 represent the fluorescence intensity in the presence and absence of thiram, respectively.

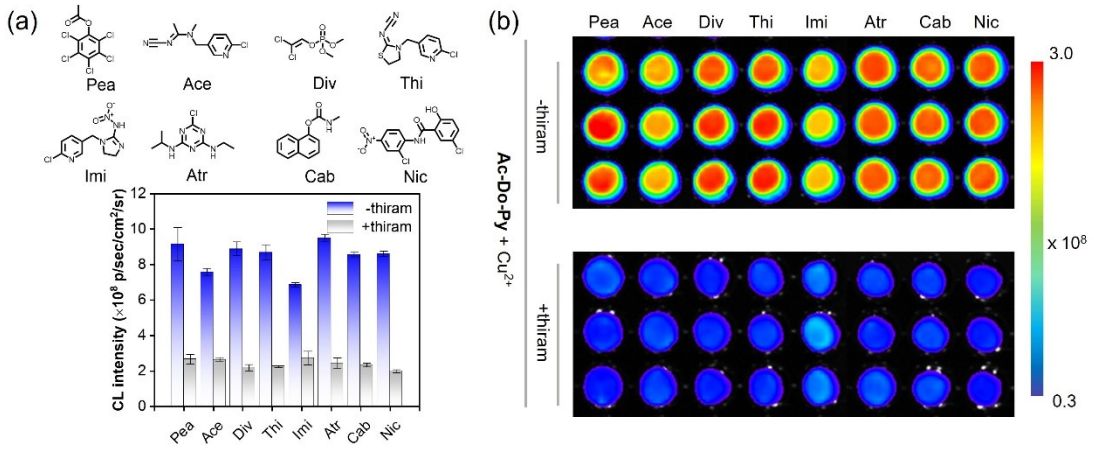

Fig. S14 (a) Structures of eight pesticides and the corresponding quantification of chemiluminescence intensity. (b) Chemiluminescence images of **Ac-Do-Py** (5 μM) incubated with Cu^{2+} (30 μM) and different pesticides (40 μM) for 10 min, in the absence (top) and the presence (bottom) of thiram (40 μM). Abbreviations: Pea = pentachlorophenol acetate, Ace = acetamiprid, Div = dichlorvos, Thi = thiacloprid, Imi = imidacloprid, Atr = atrazine, Acm = carbaryl, and Nic = niclosamide.

Table S1. Comparison of the methods for detection of thiram

Materials	Methods	LOD (μM)	Ref.
CDs-Ag^{+}-based SA hydrogel	Fluorescence	0.017	(6)
Ag-AuNDs	SERS	0.358	(7)
Ag@CDS	SERS	0.1	(8)
B-QDs/G-QDs/R-QDs	Fluorescence/Colorimetry	0.073/0.142	(9)
N-CQDs/CuNCs	Ratiometric fluorescence	0.0075	(10)
GSH-Fe nanozyme	Colorimetry	0.125	(11)
Schaap's dioxetane-based organic probe	Fluorescence/Chemiluminescence	3.5/0.1	This work

4. ^{1}H NMR and ^{13}C NMR Spectra

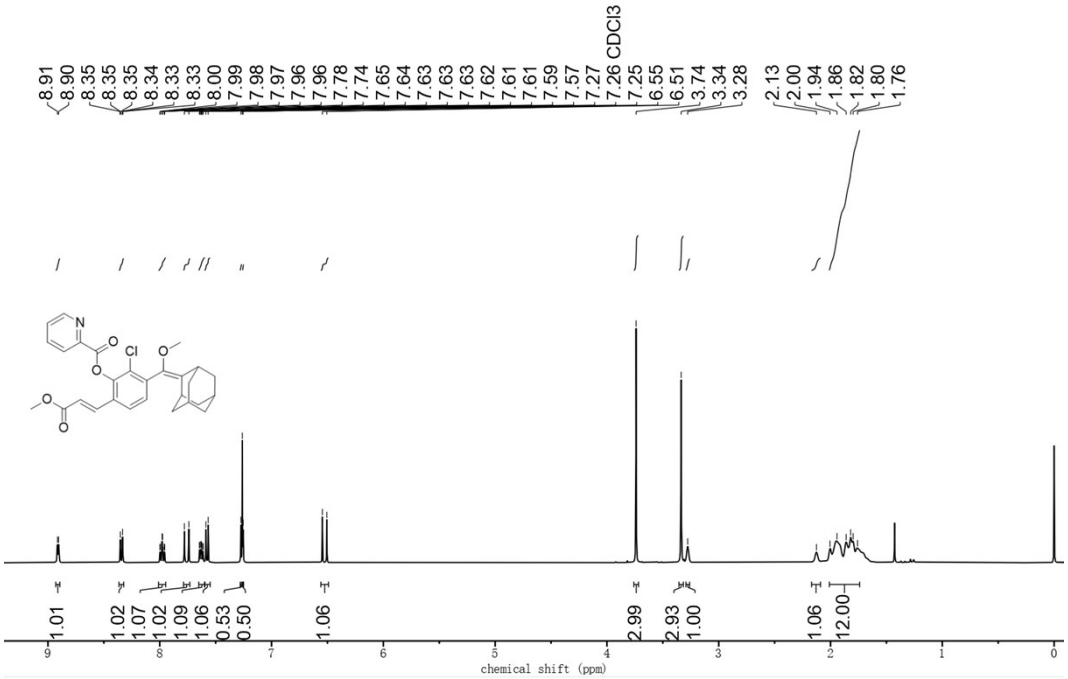

Figure S15 ^{1}H NMR spectrum of **Ac-Py** in $CDCl_3$.

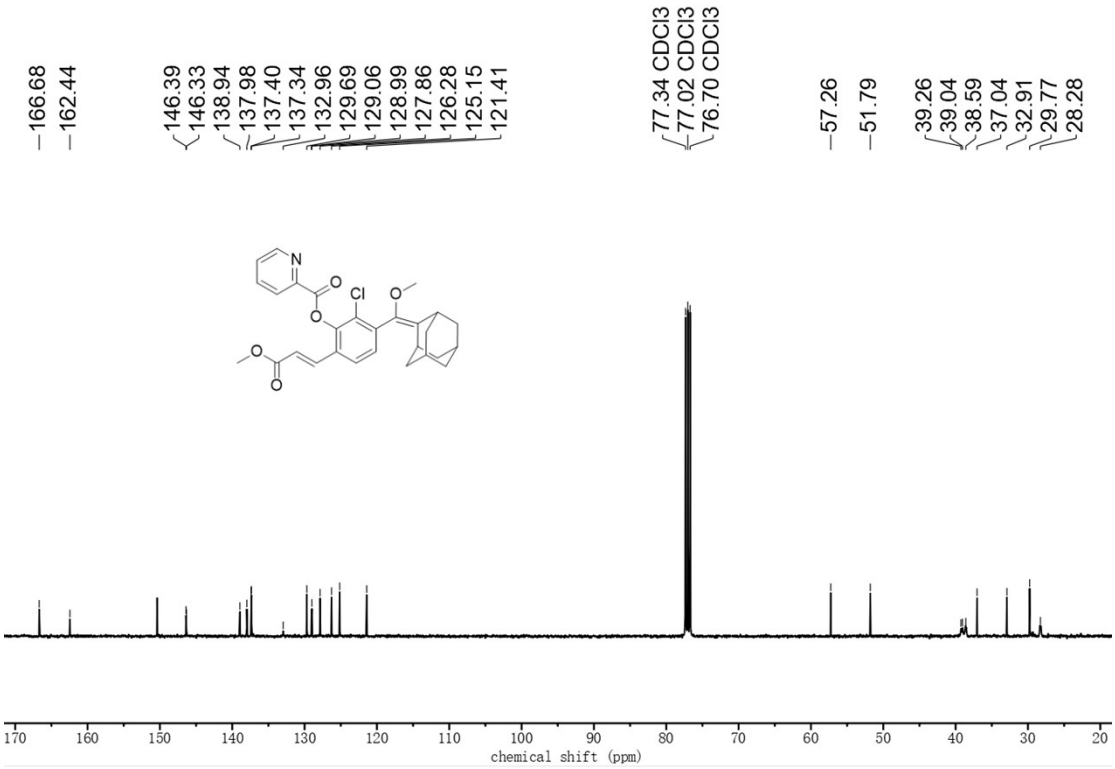

Figure S16 ^{13}C NMR spectrum of **Ac-Py** in $CDCl_3$.

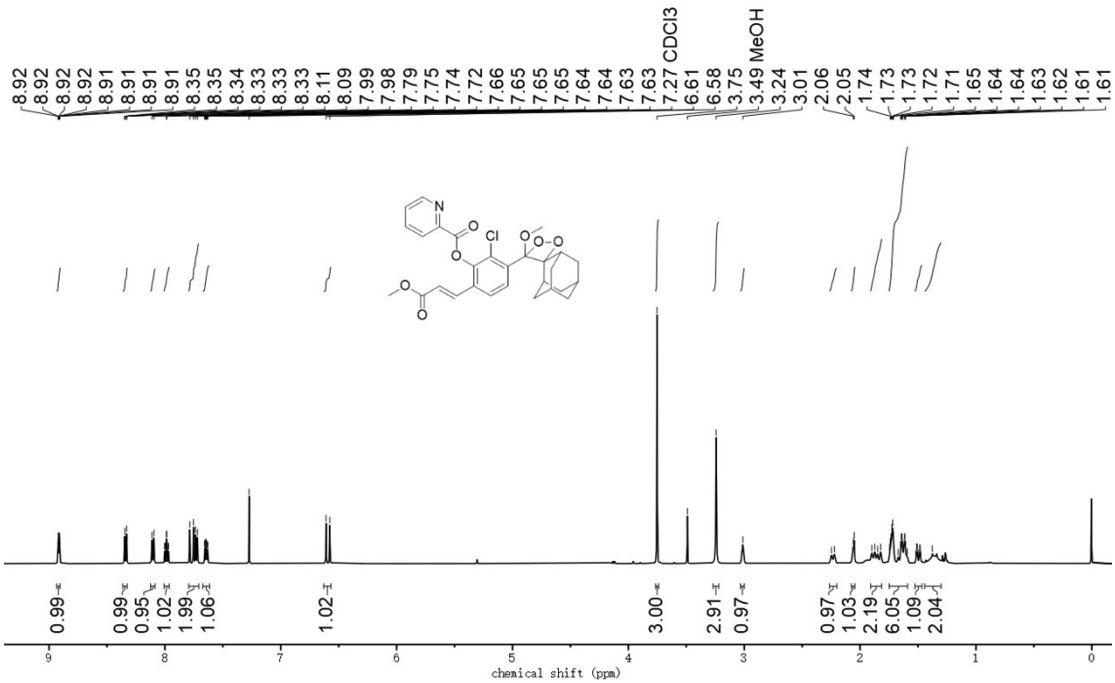

Figure S17 ^{1}H NMR spectrum of **Ac-Do-Py** in $CDCl_3$.

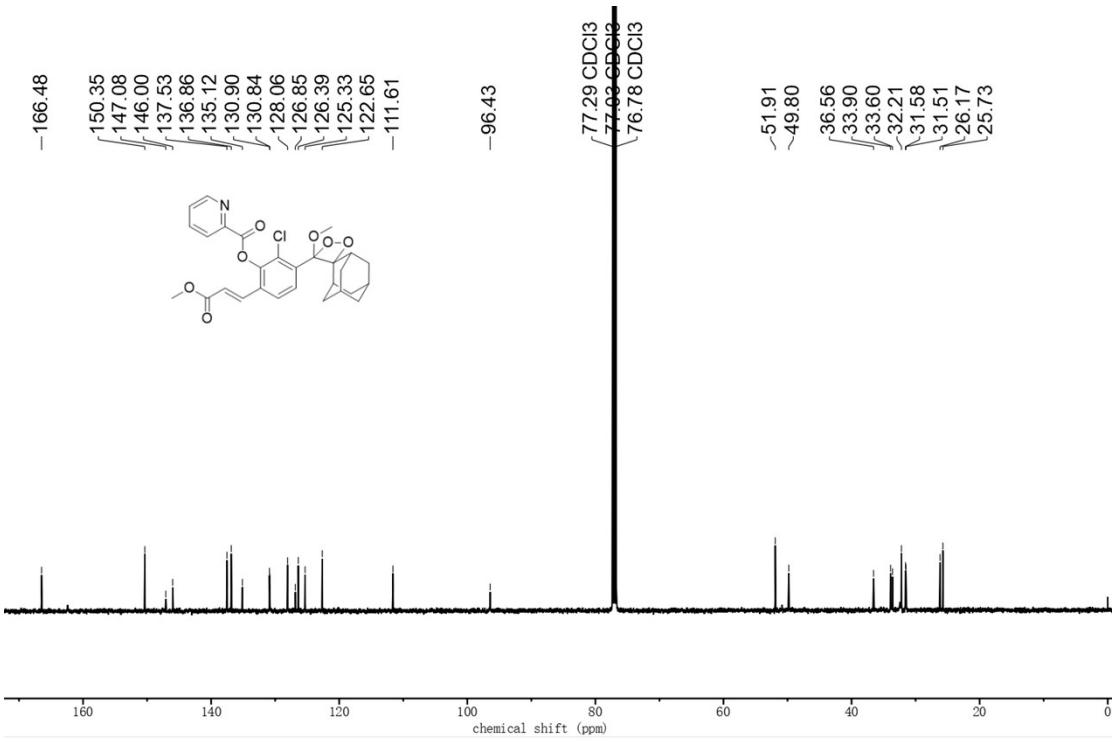

Figure S18 ^{13}C NMR spectrum of **Ac-Do-Py** in $CDCl_3$.

References

(1) M. J. Frisch, G. W. Trucks, H. B. Schlegel, G. E. Scuseria, M. A. Robb, J. R. Cheeseman, G. Scalmani, V. Barone, G. A. Petersson, H. Nakatsuji, X. Li, M. Caricato, A. V. Marenich, J. Bloino, B. G. Janesko, R. Gomperts, B. Mennucci, H. P. Hratchian, J. V. Ortiz, A. F. Izmaylov, J. L. Sonnenberg, D. Williams-Young, F. Ding, F. Lipparini, F. Egidi, J. Goings, B. Peng, A. Petrone, T. Henderson, D. Ranasinghe, V. G. Zakrzewski, J. Gao, N. Rega, G. Zheng, W. Liang, M. Hada, M. Ehara, K. Toyota, R. Fukuda, J. Hasegawa, M. Ishida, T. Nakajima, Y. Honda, O. Kitao, H. Nakai, T. Vreven, K. Throssell, Jr. J. A. Montgomery, J. E. Peralta, F. Ogliaro, M. J. Bearpark, J. J. Heyd, E. N. Brothers, K. N. Kudin, V. N. Staroverov, T. A. Keith, R. Kobayashi, J. Normand, K. Raghavachari, A. P. Rendell, J. C. Burant, S. S. Iyengar, J. Tomasi, M. Cossi, J. M. Millam, M. Klene, C. Adamo, R. Cammi, J. W. Ochterski, R. L. Martin, K. Morokuma, O. Farkas, J. B. Foresman, D. J. Fox, *Gaussian 16, Revision C.01. Gaussian, Inc., Wallingford, CT*, 2019.

(2) T. Lu, F. Chen, *J. Comput. Chem*. 2012, **33**, 580.

(3) 11）T. Lu, *J. Chem. Phys*. 2024, **161**, 082503.

(4) W. Humphrey, A. Dalke, K. Schulten, *J. Mol. Graphics* 1996, **14**, 33.

(5) N. Hananya, J. Reid, O. Green, M. Sigman, D. Shabat, *Chem. Sci*. 2019, **10**, 1380-1385.

(6) H. Li, Y. Hu, Z. Lin, X. Yan, C. Sun, D. Yao, *Food Chem*., 2024, **460**, 140405

(7) Y. Sun, X. Zhai, Y. Xu, C. Liu, X. Zou, Z. Li, J. Shi, X. Huang, *Food Control* 2021, **122**, 107772.

(8) Y. Shen, Q. Ou, Y. Q. Yang, W. W. Zhu, S. S. Zhao, X. C. Tan, K. J. Huang, J. Yan, *Talanta* 2025, **284**, 127233.

(9) Z. Lu, M. Chen, M. Li, T. Liu, M. Sun, C. Wu, G. Su, J. Yin, M. Wu, P. Zou, L. Lin, X. Wang, Q. Huang, H. Yin, H. Rao, X. Zhou, J. Ye, Y. Wang, *Chem. Eng. J*., 2022, **439**, 135686.

(10) L. Chen, J. Lu, M. Luo, H. Yu, X. Chen, J. Deng, X. Hou, E. Hao, J. Wei, P. Li, *Food Chem*., 2022, **379**, 132139

(11) X. Yan, R. Zou, Q. Lin, Y. Ma, A. Li, X. Sun, G. Lu, H. Li, *Food Chem*., 2024, **452**, 139569.